DFUB 11/97
September 1997

MULTIHADRON PRODUCTION IN HIGH-ENERGY e^+e^- COLLISIONS

GIORGIO GIACOMELLI and ROBERTO GIACOMELLI
Dipartimento di Fisica dell'Università di Bologna and INFN, Sezione di Bologna
Viale C. Berti Pichat 6/2, 40127 Bologna, Italy
E-mail: giacomelli@bo.infn.it, giacomellir@bo.infn.it

Invited paper at the 1997 Int. Conf (VIIth Blois Workshop) on elastic and diffractive scattering, Seoul, Korea

ABSTRACT. The main experimental features of multihadron production in high energy e^+e^- collisions at LEP-100 and LEP-200 are presented. In particular we consider the energy dependence of cross sections and the running of α_s. From data at LEP-100 it has been possible to determine the differences between quark-jets and gluon-jets and the main features of Bose-Einstein correlations.

1 Introduction

In this paper will be summarized and discussed some of the recent experimental results in $e^+e^- \to$ multihadron production at LEP-100 ($\sqrt{s}$ ~91 GeV) and at LEP-200 (133-183 GeV) [1-5]. Data at LEP-100 have been used to study the differences between quark-jets and gluon-jets, and Bose-Einstein correlations. LEP-200 data have been used to study the energy dependence of the multihadronic cross section, of the $e^+e^- \to W^+W^-$ cross section, of the average charged multiplicity and the running of the strong coupling constant α_s; these data also allow the determination at the highest e^+e^- c.m. energies of the event structure and of the inclusive single particle production features. The results are discussed in terms of phenomenological models, in terms of quarks and gluons and of perturbative QCD. A review of several aspects of this physics at $\sqrt{s} = m_Z$ was reported in a previous Blois meeting [6].

2 Experimental

LEP is an e^+e^- collider located in an underground tunnel of about 27 km circumference, at an average depth of about 100 m. Four large 4π general purpose detectors (ALEPH, DELPHI, L3 and OPAL) are operating simultaneously. Each of them is made of many subdetectors, with cylindrical symmetry; starting from the inner ones, one has: refined microvertex and tracking subdetectors with $\mathrm{d}E/\mathrm{d}x$ capability, located in a strong magnetic field; then follow time-of-flight systems, electromagnetic and hadron calorimeters, and muon subdetectors. The redundant trigger systems allow hadron detection with efficiencies larger than 99%. Precision "luminometers", based on $e^+e^- \to e^+e^-$ elastic scattering at small angles, allow luminosity measurements with precisions of better than 0.1% at LEP-100.

LEP-100 became operational in 1989; in runs at c.m. energies at or close to the Z^0 peak it yielded approximately 4.5 million multihadronic events per experiment, corresponding to an integrated luminosity of about 180 pb^{-1} per experiment. Data at 91 GeV have also been

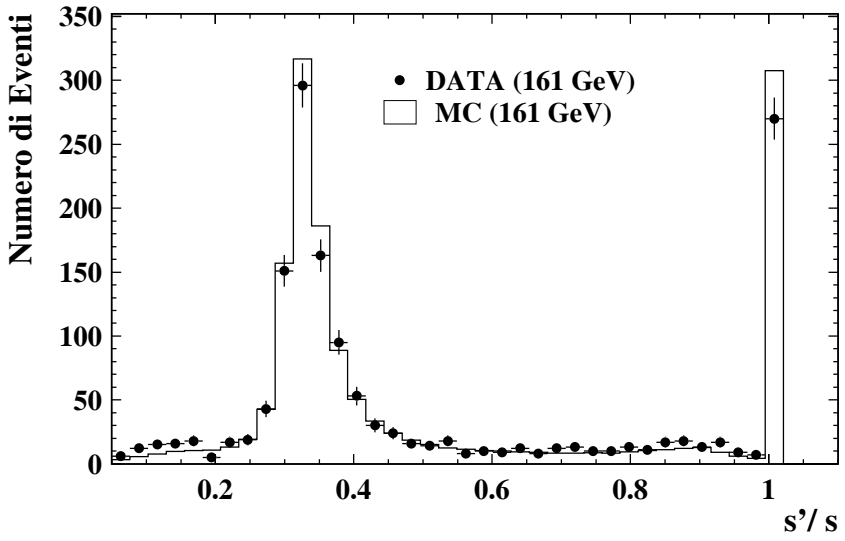

Figure 1: The number of multihadrons vs the ratio of the reduced energy $\sqrt{s'}$ to the nominal c.m. energy $\sqrt{s}$ for $e^+e^- \to q\overline{q}(\gamma)$ at 161 GeV. The points are the data, the histogram the Monte Carlo prediction.

obtained by the SLD detector operating at the SLC linear collider at SLAC. It is worth pointing out that this accelerator is capable of yielding longitudinally polarized beams.

From 1995 data have been obtained at c.m energies of 133, 161 and 172 GeV, with the limited integrated luminosities of about 5.3, 10 and 10 pb^{-1}, respectively; the 1997 running is yielding data at 183 GeV, about 6 pb^{-1} until now. 1000-1500 multihadron events have been collected at the each energy. Most hadron data at 91 GeV have the structure of two back-to-back jets of hadrons, corresponding to the reaction $e^+e^- \to \gamma/Z \to q\bar{q} \to 2$ jets; clearly there are also multi-jet events. At higher energies there is a large probability for photon-radiation from the initial electron or positron; this radiation lowers the effective c.m. energy of the colliding e^+e^- and it leads to asymmetric situations whereby the two produced jets (or the produced lepton pair) are not produced back-to-back. The effective c.m. energy after radiation from the initial state is shown in Fig. 1: notice the "radiative return" to the Z^0 [1]. Events may be selected at the nominal c.m. energy (equal to twice the beam energy) with an appropriate cut in the reduced energy variable $\sqrt{s'}$. After selection cuts one has about 300 multihadron events per LEP experiment and per energy.

In what follows we shall mainly report on data obtained by the OPAL experiment; the other experiments have obtained similar results, some of which are reported here.

3 Energy dependence of cross sections

Fig. 2 shows the energy dependence of the multihadronic cross sections without removing and removing the radiative events; the standard model (SM) predictions (lines) are in good agreement with the data (points) [1]. The figure also shows the data and the predictions for the leptonic channels, $e^+e^- \to l^+l^-(\gamma)$.

Fig. 3 shows the energy dependence of $R_b = \Gamma_b/\Gamma_h$ [1]. This ratio was measured with high precision at $\sqrt{s} \simeq$91 GeV, while the statistical precision is poor at higher energies. The

measured values are in agreement with the predictions of the SM (solid line). The difference which existed in the old measurements of R_b at the Z^0 mass peak seems now to have been reduced and probably disappeared. Future high statistics measurements at higher energies should yield new tests of the SM.

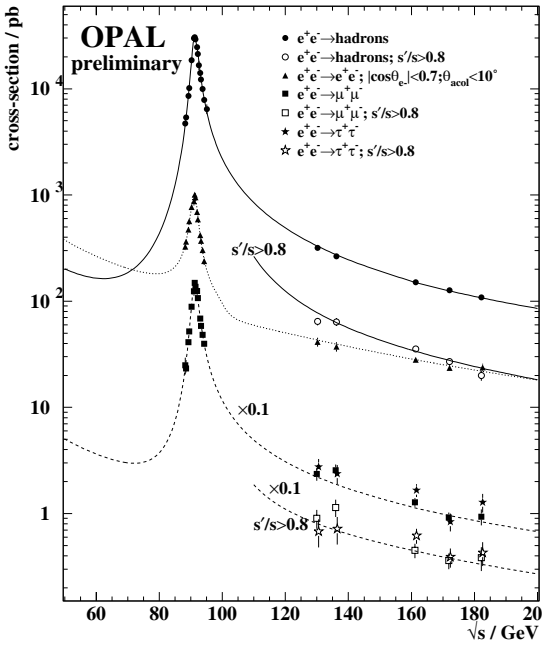

Figure 2: Cross sections vs c.m. energy.

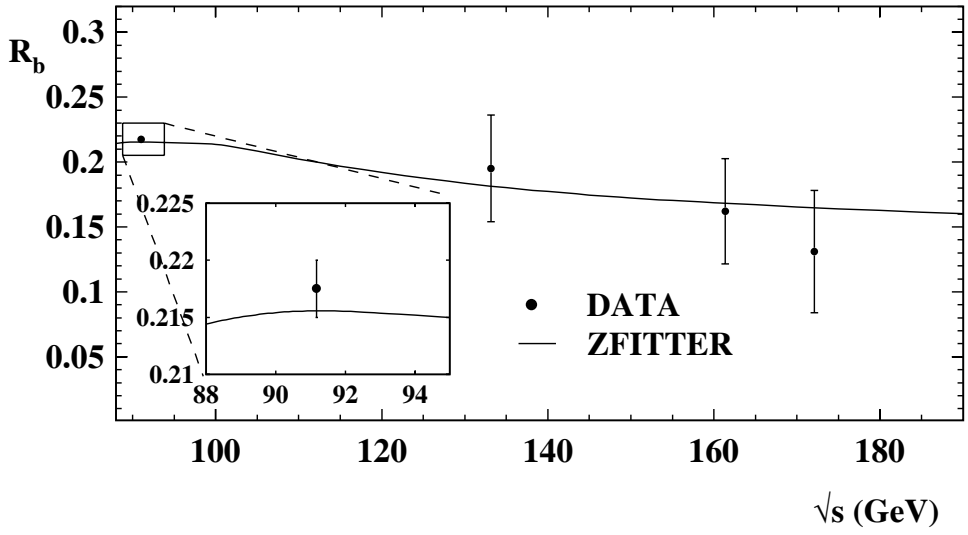

Figure 3: Energy dependence of $R_b \to \Gamma_b/\Gamma_h$. The points are data, the line is the prediction of the SM.

4π detectors allow a relatively simple determination of the charged multiplicity dis-

tribution and of its moments. The data correction procedure is based on Monte Carlo simulations. Even with limited statistics one obtains a reasonable charged multiplicity distribution. The multiplicity distributions determined at different energies, when plotted as $\overline{n_{ch}}P_{n_{ch}}$ versus $n_{ch}/\overline{n_{ch}}$ superimpose ($\overline{n_{ch}}$ is the average charge multiplicity); this is a manifestation of the so called KNO scaling, which seems to be valid up to the highest LEP energies. The measurements of the multiplicity distributions at higher energies and with higher precisions will eventually allow better tests of KNO scaling.

From the multiplicity distributions one can calculate the moments of the distributions, in particular $\overline{n_{ch}}$ and the ratio $\overline{n_{ch}}/D$, where D is the dispersion. This last ratio seems to be independent of energy and is equal to $\overline{n_{ch}}/D = 3.12 \pm 0.05$ (DELPHI).

The energy dependence of the average charged multiplicity is shown in Fig. 4 [1]. The data have been fitted to an empirical function

$$\overline{n_{ch}} = A + B \ln s + C \ln^2 s \tag{1}$$

(obtaining $A \simeq 3.3$, $B \simeq -0.4$, $C \simeq 0.26$) and to a form obtained from QCD in the NLLA approximation

$$\overline{n_{ch}} = a + \alpha_s^b + e^{c/\sqrt{\alpha_s}} \tag{2}$$

where b, c are constants given by QCD; $\alpha_s(s)$ has the standard energy dependence on Λ. a and Λ are determined from the fit of the data to Eq. 2, obtaining a=0.062±0.009, Λ=(124±41) MeV. Another multiplicative term is often added in Eq. 2, $(1+d\sqrt{\alpha_s})$. With the present precision all the various fits adequatly describe the available data, see Fig. 4.

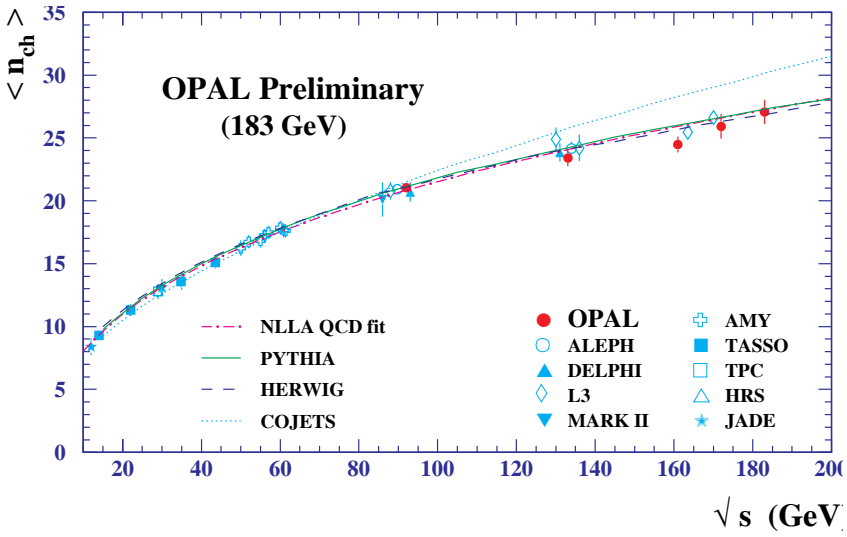

Figure 4: Average charged multiplicity vs c.m. energy. The lines represent different fits to the data.

4 General multihadronic features

Event shape variables. Several variables have been introduced to characterize the struc-

ture of multihadron (MH) events; we shall only recall the following:

$$\text{Thrust} \qquad T = \text{Max}\frac{\Sigma_i(\vec{p_i}\cdot\vec{n})}{\Sigma_i|\vec{p_i}|} \tag{3}$$

$$\text{Sphericity} \qquad S = 1.5\ \text{Min}\frac{\Sigma_i p_{i\perp}^2}{\Sigma_i {p_i}^2} \tag{4}$$

Events with two opposite jets of hadrons have T=1, S=0; spherical MH events have T=1/2, S=1. The measured distributions in T and in S of the multihadrons show the predominance of two-jet events, and are in good agreement with the Monte Carlo predictions. It has to be noted that the Monte Carlos were optimized using event shape variables at $\sqrt{s} = m_Z$.

Parameters for each produced hadron. The variables used in hadron collisions are also used in positron-electron collisions, but are here defined with respect to the Thrust axis. The variables include the transverse and longitudinal momenta, and

$$\text{Rapidity} \qquad y = \ln\frac{\vec{p_k}\cdot\vec{n_T} + E_k}{\vec{p_k}\cdot\vec{n_T} - E_k} \tag{5}$$

$$x_p - \text{variable} \qquad x_p = p_k/p_{\text{beam}} \simeq 2p_k/\sqrt{s} \tag{6}$$

$$\xi_p - \text{variable} \qquad \xi_p = \ln(1/x_p) \tag{7}$$

Fig. 5 shows the distribution in rapidity at $\sqrt{s}$=172 GeV. The Monte Carlo predictions are once again in agreement with the experimental data. Fig. 6 shows the energy evolution of the distribution in the ξ_p-variable (DELPHI data).

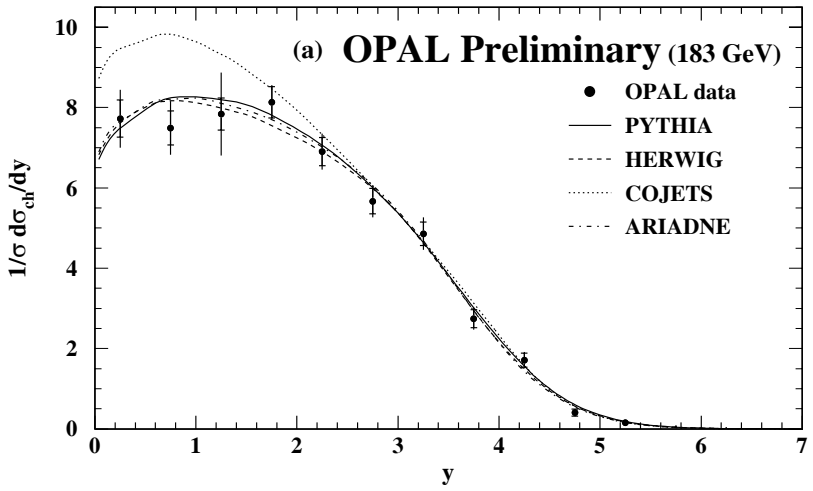

Figure 5: Distribution in rapidity, y, for charged particles at $\sqrt{s}$=183 GeV, compared with the predictions of different Monte Carlos.

Average number of identified hadrons per event. Charged hadrons are identified via momentum and dE/dx measurements; DELPHI uses also RICH Cerenkov counters, thus covering a larger fraction of phase space. ${K^0}'s$ and ${\Lambda^0}'s$ are identified via their characteristic decays inside the tracking chambers. Resonances are identified from their decay products.

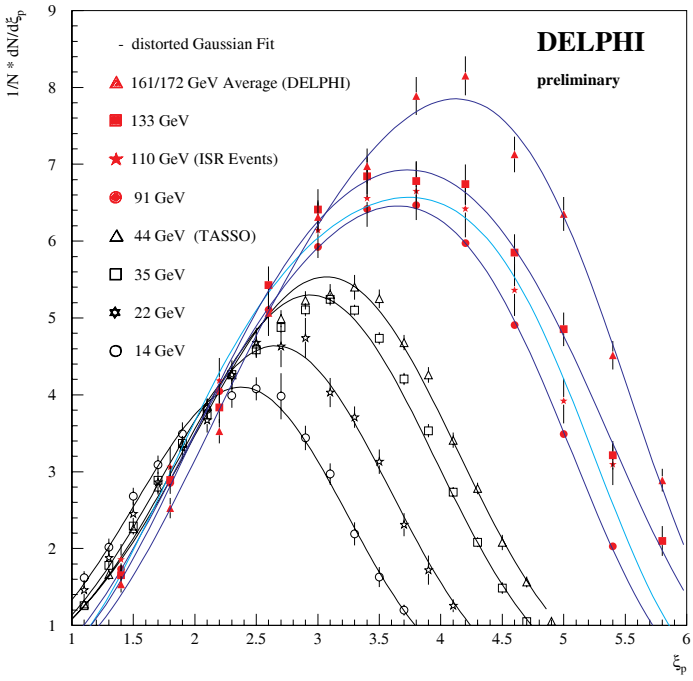

Figure 6: Distribution in $\xi_p = \ln(1/x_p)$ for charged particles at different c.m. energies.

Over 35 states have been thus far identified, and their production rates measured. One has at $\sqrt{s}$=91.2 GeV (OPAL data):
$\overline{n} = \overline{n_{ch}} + \overline{n_{neut}} = 20.9 + 10.5 = 8.5\pi^+ + 8.5\pi^- + 9.8\pi^0 + 1.2K^+ + 1.2K^- + 1.0K^0 + 1.0\overline{K^0} + 0.98p + 0.98\overline{p} + 0.37\Lambda^0 + 0.10\Sigma^+ + 0.074\Sigma^0 + 0.08\Sigma^- + ...$
Most of the measured produced rates are well predicted by the Monte Carlos; but for the Λ^0, Ξ^-, $\Sigma(1385)^+$, $\Xi(1530)$, Ω^- the predicted rates differ from the measured ones by more than three standard deviations.

A simple thermodynamical model with two produced "fireballs" moving in the directions of the final two jets of hadrons reproduces well most of the measured production rates, see Fig. 7 [7]. Notice that the main dependence is exponential in mass, $n_{ch} \sim e^{-m_h/T}$. The model has three parameters, for each of the two fireballs: the temperature T=160 MeV, the volume of the hadron gas $v \simeq 20$ fm and a strangeness suppression factor $\gamma_s \simeq 0.7$. The model yields negative binomials for the charged hadron multiplicity distributions.

5 Some QCD features

In this section we shall discuss some of the important experimental aspects of QCD recently studied at LEP: the running of α_s and the determination of the differences between hadron jets from quarks and gluons. Precision tests of the Standard Model (SM) have been repeated each year with new data and increased precision [5].

α_s. At each LEP energy the strong coupling constant α_s has been determined by a variety of methods, in particular from fits of the QCD predictions to a number of corrected dis-

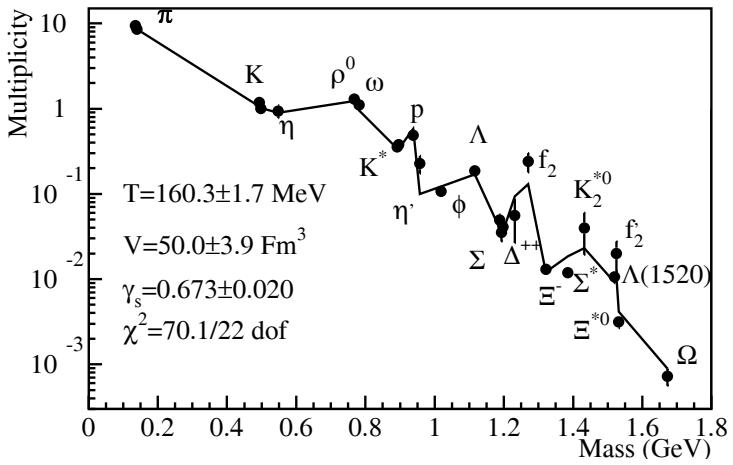

Figure 7: Average number of hadrons per MH event vs mass. The line is the prediction of the thermodynamic model with two fireballs.

tributions, for (1-T), D , etc. and from $R_l = \Gamma_h/\Gamma_l$. The theoretical QCD descriptions of these observables are calculated at $O(\alpha_s^2)$+ NLLA. For R_l one has

$$R_l = R_l^0(1+\delta_{QCD}) = R_l^0[1 + c_1\alpha_s/\pi + c_2(\alpha_s/\pi)^2 + \ .....] \tag{8}$$

At each energy a combined result from each experiment is computed using a weighted average procedure; the total error on the determination is computed by adding in quadrature all uncertainties, both for a single determination and for the combined value. When evolved to the scale m_Z one obtains consistent values, with the most precise value measured at m_Z. In Fig. 8 is shown a compilation of measurements of α_s; the solid curve shows the $O(\alpha_s^3)$ prediction for α_s(Q) using $\alpha_s(m_Z)$=0.118±0.006 [1]. The compilation clearly proves the running of α_s, as required by QCD.

The flavour independence of α_s was verified in a number of measurements at LEP-100. **Jets from quarks and from gluons.** Many studies have been done at LEP to establish the differences between a quark jet and a gluon jet. For this purpose one first selected three-jet events in a *Y configuration*, where the low energy quark and gluon jets are at 150° with respect to the high energy quark jet, and the *"Mercedes events"* where the three jets are at 120° from each other. From these measurements it was established that with respect to the light quark jet the gluon jet is broader, has a larger hadron multiplicity and yields hadrons with a softer energy spectrum. These conclusions were only qualitative and could not be compared with a precise QCD calculation. The reaction $e^+e^- \to \gamma/Z \to q\overline{q}$ leads to a $q\overline{q}$ from a color singlet source; this situation cannot be obtained for gluons in the above described geometries for three-jet events. The above measurements are not inclusive, they use a jet finder algorithm and the gluon jet cannot be a color singlet. The QCD calculations cannot reproduce the experimental situations. Moreover the theory stops at the parton level, while the experiments are at the hadron level.

Recent measurements selected rare events for which inclusive measurements could be made, thus avoiding most of the above mentioned difficulties. The selected events contain two tagged light quarks in one hemisphere, say the left one: all hadrons in the left hemisphere

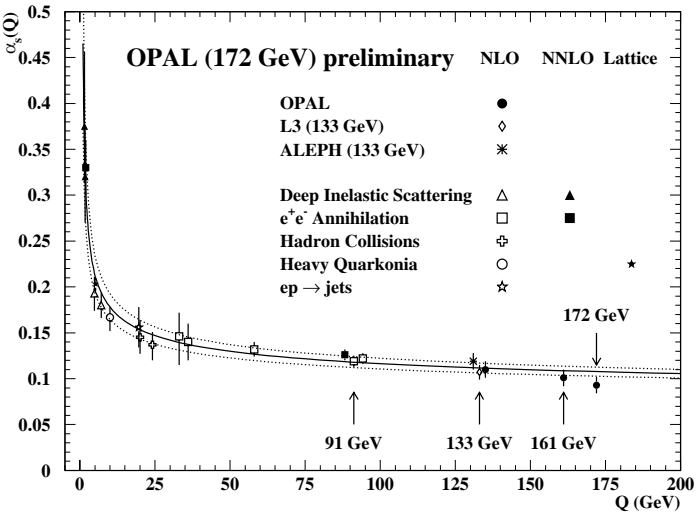

Figure 8: Variation of α_s with $Q = \sqrt{s}$. The labels NLO and NNLO refer to the order of calculations used. NLO corresponds to $O(\alpha_s^2)$, and NNLO to $O(\alpha_s^3)$. The curves are $O(\alpha_s^3)$ QCD predictions.

are assumed to come from the two quarks, which at the limit are collinear. The gluon goes in the right hemisphere, and at the limit is collinear with the two quarks, and one attributes all the hadrons in the right hemisphere to the gluon jet. The measurements yield the charged multiplicity distributions shown in Fig. 9 [8]. For 39 GeV gluons the ratio of the average charged multiplicities is:

$$r_{ch} = \frac{< n_{ch} >_g^{incl}}{< n_{ch} >_{uds}^{hemisphere}} = \frac{14.5}{10.1} = 1.49 \pm 0.03 \pm 0.05 \qquad (9)$$

The theoretical calculation using analytic NNLO with approximate energy conservation and corrected via Monte Carlo to go from the parton level to the hadron level gives a value close to the measured one. Further theoretical work should eventually yield an even better agreement.

6 Bose-Einstein correlations

The size of the region from where pions originate in high-energy collisions may be determined from the study of second-order (intensity) interference effects between identical pions (Bose-Einstein (BE) correlations). The interference originates from the ambiguity in the paths of the two pions, and manifests itself in an enhancement of the number of identical pions (like-charge pairs) when they are close in phase space. We shall use the notation in terms of the four-momentum transfer $Q = -(p_1 - p_2)^2 = m_{\pi\pi}^2 - 4m_\pi^2$ of the particle pairs; $m_{\pi\pi}$ is the invariant mass of the pair, assuming both particles to be pions. The distribution in Q of like-charge pairs has to be normalized to a Q-distribution which does not contain BE correlations, for instance the distribution of unlike-charge pairs:

$$C(Q) = (N^{++} + N^{--})/N^{+-} \qquad (10)$$

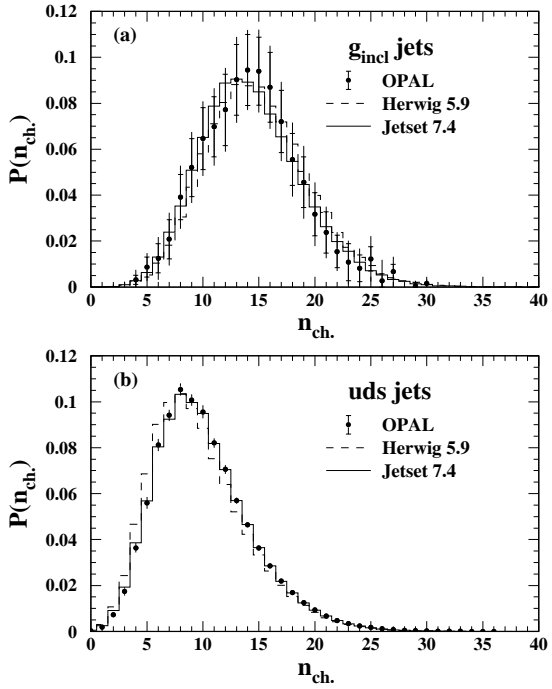

Figure 9: Multiplicity distributions of the hadrons produced in uds quark-jets and in gluon-jets.

Various theoretical parametrizations are used in the literature to interpret the data. We shall use the Goldhaber parametrization:

$$C(Q) = N(1 + \lambda e^{-\alpha^2 R^2})(1 + \delta Q) \tag{11}$$

N is a normalization factor, λ is the "chaoticity parameter" (λ=0 for no BE interference, λ=1 for maximum BE interference), R is the radius of the emitting region, and δ is a parameter which takes into account the background. Fig. 10 shows the Q-dependence of C(Q) for ch-ch pairs: a clear enhancement is observed at small values of Q [9]. Fits of the data to the function (11), eliminating the regions with resonances in the reference N^{+-} distribution, yield $R \simeq 1$ fm; this radius seems to be energy independent.

More recently the three pion BE correlations have been measured by DELPHI and by OPAL. It seems that the 3 pion emitting radius is smaller than the 2 pion one.

OPAL analyzed the dependence of the 2 pion emitting region from the average charged multiplicity of the multihadron events. It found an increase of the radius with n_{ch} (Fig. 11), while the chaoticity parameter λ decreases [9].

7 The reaction $e^+e^- \to W^+W^-$

In 1996 LEP started running at energies above the W-pair threshold ($\sqrt{s} = 2m_W$). This allows to perform precision W-physics and to test the triple boson vertex ZWW of the Standard Model. The most important diagrams for W-pair production are the s-channel γ/Z exchange, and the t-channel neutrino exchange. The first available LEP energy, 161

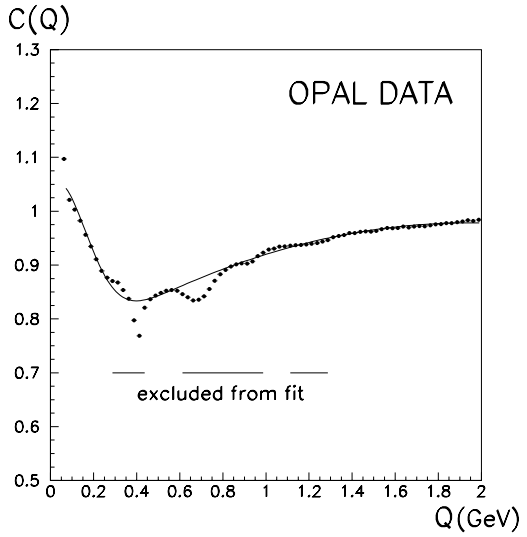

Figure 10: Bose-Einstein correlation function C(Q) vs Q for charged particle pairs.

GeV, is just above the W-pair production threshold, and the cross section has a particularly strong dependence on the value of the mass of the W-boson; it is thus possible to extract m_W from the data by measuring the cross-section and comparing its value with theoretical predictions in the context of the SM. At higher energies the measurement of the W mass can be made by direct reconstruction of the invariant mass of the fermion pair for each W decay channel.

Fig. 12 shows the energy dependence of the W^+W^- cross section measured at the three energies of 161, 172 and 183 GeV: it has the tipical dependence of a reaction at its threshold. The measured values are consistent with the SM predictions. Anomalous triple gauge couplings can affect both the total production cross section and the shape of the differential cross-section as a function of the W production angle. No deviations have been observed and one can thus place only upper limits for anomalous couplings.

8 Conclusions

The four LEP experiments provided precise data on charged multiplicities, global and detailed properties of multihadronic events at energies close to the Z peak and more recently with smaller precisions, at 130-183 GeV. The data are interpreted in the context of the multi-jet structure of the events; a two-fireball thermodynamic model also explains some of the data. The experimentally observed features seem to be included in the various Monte Carlos, which were optimized at the Z peak. Bose-Einstein correlations have been studied for charged and neutral particle pairs and also for three charged particles. The radius of the emitting region is consistently of the order of 1 fm. The dependence of the emitting radius on the charged hadron multiplicity has been established. The large amount of data at the Z resonance allows the study of detailed fundamental features, like the difference between quark-jets and gluon-jets. The higher LEP-200 energies allow to study the variation of α_s on a larger energy range. Moreover the high energies available now for the first time allow

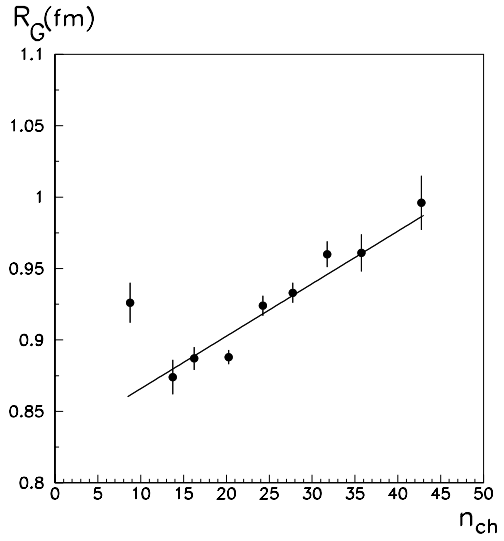

Figure 11: BE correlations: dependence of the emitting radius R on n_{ch} [9].

to study the threshold behaviour of $\sigma(e^+e^- \to W^+W^-)$, a precise determination of the W boson mass, and a test of the triple boson vertex ZWW.

We would like to thank the members of the OPAL Collaboration for their cooperation.

9 References

1. OPAL Collaboration, K.Ackerstaff et al. *(QCD studies with e^+e^- annihilation data at 172 GeV)* OPAL-PN281 (1997); *(Initial studies of hadronic events at 183 GeV at LEP2)* OPAL-PN315 (1997); *(Production of fermion-pair events in e^+e^- collisions at 182 GeV c.m. energy)* OPAL-PN316 (1997).
2. ALEPH Collaboration *(Preliminary ALEPH results at 183 GeV)* 1997 EPS-HEP Conf., Jerusalem, paper 856.
3. L3 Collaboration, M.Acciarri et al. *(Preliminary results from the L3 Experiment at 183 GeV)* Paper presented at the 1997 EPS-HEP Conf, Jerusalem; *(Study of hadronic events and test of QCD)* Paper presented at the 1997 EPS-HEP Conf, paper 122.
4. DELPHI Collaboration, J.Drees et al. *(QCD results from the DELPHI measurements at 161 GeV and 172 GeV)* DELPHI 97-92, CONF 77 (1997); *(Charged particle multiplicity distribution in $e^+e^- \to q\overline{q}$ events at 161 and 172 GeV and from the decay of the W boson)* DELPHI 97-78, CONF 64 (1997).
5. LEP2 Standard Model group *(Tests of the Standard Model and constraints on new physics from measurements of fermion-pair production at 130-172 GeV at LEP)* CERN-PPE/97-101 (1997).
6. G.Giacomelli *(Multiplicities, intermittency, average transverse momentum, and Bose-Einstein correlations at LEP)* Nucl.Phys. B (Proc. Suppl.) 25 (1992) 30, DFUB 91/17 (1991).
7. F.Becattini *(Universality of thermal hadron production in pp, $\bar{p}p$ and e^+e^- collisions)* DFF 263/12/1996.
8. OPAL Collaboration, K.Ackerstaff et al. *(Multiplicity distributions of gluon and quark jets and tests of QCD analytic predictions)* CERN-PPE/97-105 (1997).
9. OPAL Collaboration, G.Alexander et al. *(Multiplicity dependence of Bose-Einstein correlations in hadronic Z^0 decays)* Z.Phys. C72 (1996) 389; L3 Collaboration, M.Acciarri et al. *(Study of Bose-Einstein correlations with the L3 detector at LEP)* L3 note 2134 (1997).

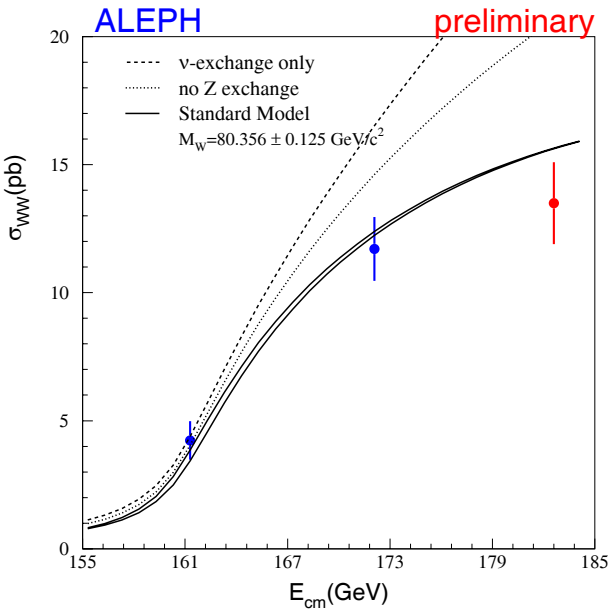

Figure 12: Cross section for the reaction $e^+e^- \to W^+W^-$ versus $\sqrt{s}$. The solid lines are the SM predictions for two values of m_W differing by ± 125 MeV. The dashed line is obtained from the t-channel neutrino exchange diagram only, the dotted line is obtained by including also the s-channel photon exchange diagram and not the Z^0-exchange one (ALEPH) [2].

10. OPAL Collaboration, K.Ackerstaff et al. *(Measurement of the triple gauge boson coupling from W^+W^- production in e^+e^- collisions at 161 GeV)* Phys.Lett. B397 (1997) 147; *(Measurement of the W boson mass and W^+W^- production and decay properties in e^+e^- collisions at $\sqrt{s}$=172 GeV)* OPAL-PN301 (1997); *(Production of W^+W^- in e^+e^- collisions at $\sqrt{s}$=181-183 GeV)* OPAL-PN313 (1997).